Charge Separation and Charge Distribution in Rearrangement Reactions of β-(Phosphatoxy)alkyl Radicals

Y. Wang,[‡] S. Grimme,[$] and H. Zipse*,[‡]

Contribution from the Department Chemie, LMU München, Butenandtstrasse 13, D-81377 München, Germany, and the Organisch-Chemisches Institut der Universität Münster, Corrensstrasse 40, D-48149 Münster, Germany

Received: December 23, 2003; In Final Form: January 8, 2004

Unimolecular reaction pathways for the 2-(dimethylphosphatoxy)-2-(*p*-methoxyphenyl)-1,1,-dimethylethyl radical **1** have been studied with several different hybrid density functional methods. The most reliable prediction has been obtained through combination of relative energies calculated at the BHLYP/6-311+G(d,p)//Becke3LYP/6-31G(d) level of theory with solvation free energies calculated with the PCM (polarizable continuum) model for THF. All reaction pathways characterized in detail have mixed homolytic/heterolytic character with a dominating heterolytic component. Concerted reaction pathways for 1,2- and 3,2-migration of the phosphate group lead to rearranged benzylic radical **2** that is more stable than **1** by about 30 kJ/mol. Also, a flat region of the potential energy surface has been identified that contains intermediates of nonintegral charge separation. This region of the potential energy surface can be reached from the reactant radical **1**, the rearranged radical **2**, and the phosphoric acid elimination products **11** and **12**. The intermediates located on this part of the potential energy surface can best be described as contact radical ion pairs based on their overall geometrical structure. However, the phosphate group charges never exceed a value of −0.75 even in THF solution. The absolute reaction barriers are strongly influenced through the presence of a solvent reaction field even for a low-polarity solvent such as THF and thus show the expected behavior for a charge-separating reaction type. The gas-phase UV−vis excitation spectrum calculated for contact radical ion pairs using the adiabatic TDDFT approximation features a very long wavelength absorption between 900 and 1000 nm absent in the spectrum of the underlying radical cation whose longest wavelength absorption is predicted to be at 555 nm. The results of the TDDFT computations have been confirmed by coupled-cluster calculations employing the CC2 approximation.

Introduction

The chemistry of β-(phosphatoxy)alkyl radicals has been studied intensely in recent years because of the involvement of these species in decomposition reactions of DNA and other organophosphates.[1−4] The currently accepted consensus mechanism involves formation of a contact ion pair (Scheme 1) whose fate depends on the substitution pattern as well as the reaction medium. Although dissociation of the initially formed contact ion pair and trapping of the radical cation product by solvent or other nucleophiles prevails in polar solution, recombination to either the initial or a rearranged radical dominates the reaction in apolar organic solvents. In appropriately substituted systems intramolecular trapping by nucleophiles has also been observed.[5] Theoretical studies of rearrangement reactions of β-(phosphatoxy)alkyl radicals have up to now been restricted to small model systems.[6,4f] Reaction pathways that could be identified in these latter studies include the concerted 1,2- or 3,2-phosphate rearrangement (Scheme 1, pathways a and b), the concerted syn elimination through pathway c, and the homolytic C−O bond cleavage along pathway d. Stationary points corresponding to heterolytic cleavage of the C−O bond (pathway e) could, up to now, not be identified. In order to determine whether this is due to the absence of stabilizing substituents present in most of the experimentally studied systems, we have selected here a model system **1** (R_1=R_2=CH_3, R_3=$CH_3O-C_6H_4-$) closely related to those that have been characterized in detail by Newcomb et al.[4e] The experimentally and theoretically studied systems differ only in their choice of phosphate protecting groups: while the diethyl ester has been selected in the experiment, the dimethylester has been chosen for the theoretical studies here. Time-resolved experiments for the diethyl ester in THF as the solvent proceed to give rearranged benzylic radicals (pathways a/b or e) as the sole product with an activation energy of +40.6 ± 5 kJ/mol. Reaction in acetonitrile leads to a mixture of rearranged products and radical cations whose formation appears to have an identical Arrhenius activation energy of +25.5 ± 3.8 kJ/mol. The decreased activation energy in a medium of higher polarity suggests that the rearranged products are formed either through initial formation of a contact ion pair (pathway e) or through concerted processes a and b with strongly polarized transition states.

Theoretical Methods

As in previous studies,[4f,6] all geometry optimizations were performed with the standard 6-31G(d) basis set using the Becke3LYP (B3LYP) hybrid functional.[7,8] Single-point energies have then been calculated using the larger 6-311+G(d,p) basis set with both the B3LYP as well as the Becke-half-and-half-LYP (BHLYP)[8,9] hybrid density functional. A comparison of reaction barriers for radical reactions with these two functionals has recently shown the B3LYP barriers to be somewhat too low, whereas the BHLYP barriers are slightly too high in many

[‡] Department Chemie, LMU München.
[$] Organisch-Chemisches Institut der Universität Münster.

10.1021/jp037984+ CCC: $27.50
Published on Web 02/28/2004

SCHEME 1: Mechanistic Pathways for Unimolecular Reactions of β-(Dialkylphosphatoxy)alkyl Radicals

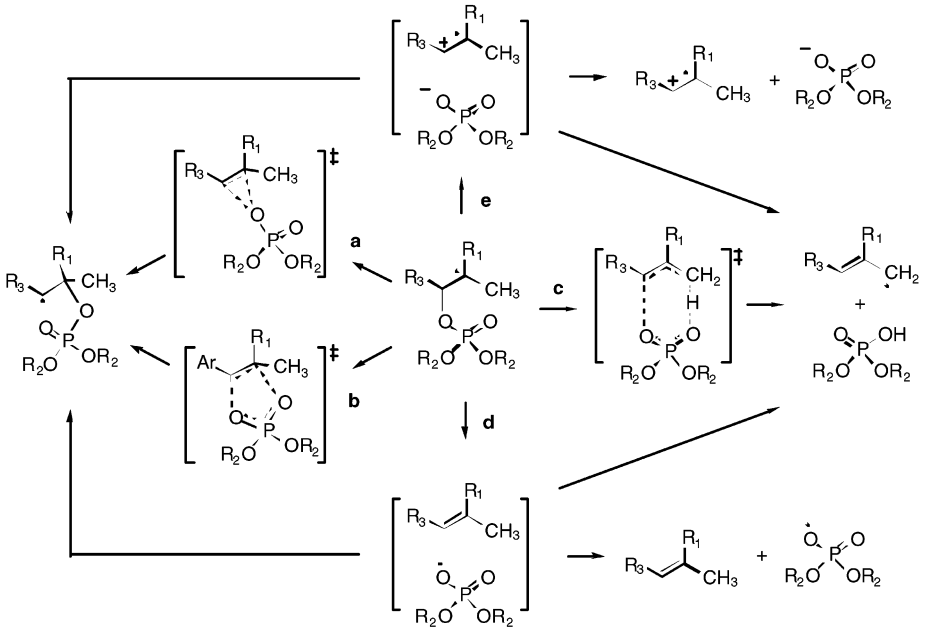

cases. We could therefore hope that the reaction barriers computed with these two functionals bracket the exact value.[10] Combination of these single-point energies with unscaled B3LYP/6-31G(d) zero-point vibrational energies yields the energies discussed in the text as "B3LYP/LB" and "BHLYP/LB". If not mentioned otherwise, all energies cited in the text refer to the B3LYP/LB level of theory. For stationary points **1**−**4** the structures have been reoptimized at the BHLYP/6-31G(d) level in order to test the influence of the functional on the geometries. Recalculation of the BHLYP/6-311+G(d,p) single-point energies on these modified geometries allows for a quantification of these effects. When differences in zero-point vibrational energies calculated at the corresponding levels of theory are included, the BHLYP/6-311+G(d,p)//BHLYP/6-31G(d) and BHLYP/6-311+G(d,p)//B3LYP/6-31G(d) relative energies differ by less than 2 kJ/mol. This suggests that the use of B3LYP/6-31G(d) geometries for the BHLYP/6-311+G(d,p) single-point calculations is most likely not the source of major errors. Atomic charges and spin densities have been calculated according to the natural population analysis (NPA) scheme using the DFT Kohn−Sham orbitals and are given in fractions of the elementary charge unit e.[11,12] The cumulative charge and spin density of the phosphate groups cited in the text have been obtained by simply summing the atomic contributions of all constituting atoms. Vertical electronic excitation spectra have been calculated using the TDDFT/RPA scheme[13] in combination with the UBecke3LYP hybrid functional and the 6-311+G(d,p) basis set using UB3LYP/6-31G(d) geometries. Earlier reports[14] on the dependence of the oscillator strength on the number of calculated states could not be confirmed as repeated calculation of the excitation spectrum with different numbers of states (between 6 and 10) gives identical results. Solvent effects have been determined using single-point calculations with the PCM (polarizable continuum) solvation method in combination with the UAHF cavity model and a tesserea area of 0.3 Å^2 at the Becke3LYP/6-31G(d) level of theory.[15] Relative energies in solution have been obtained by combining the PCM solvation free energies with either the B3LYP/LB or BHLYP/LB energy differences. All these calculations have been performed with Gaussian 98.[16] Comparative coupled-cluster response calculations employing the CC2[17] formalism and the resolution of the identity (RI) approximation for the two-electron integrals[18] have been performed with the TURBOMOLE[19] suite of programs. A polarized valence triple-ζ AO basis set (TZVP: [5s3p1d]/[3s1p])[20] and the above-mentioned DFT optimized geometries were used throughout. As in the TDDFT treatments, all calculations were performed unrestricted. The oscillator strengths were obtained in the dipole-lengths form.

Results

Gas-Phase Reaction of 2-(Dimethylphosphatoxy)-2-(*p*-methoxyphenyl)-1,1-dimethylethyl Radical (1). Most of the reaction pathways studied here originate at reactant radical **1** (Figure 1). The energetically most favorable conformation of **1** displays structural features commonly expected for a tertiary, β-substituted radical: the radical center is slightly pyramidalized by 14° and oriented such that the β-C−O bond aligns with the radical center SOMO (singly occupied molecular orbital). The C−O bond connecting the phosphate group to the styrene substructure is slightly elongated to 1.49 Å (Figure 2). Most of the unpaired spin density in **1** is localized at the C1 carbon atom with coefficient 0.85 while only a minor amount is delocalized over the phosphate group (0.06). The phosphate group does, however, carry a significant amount of negative charge (−0.37) already in radical **1**. 1,2-Migration of the dimethyl phosphate group yields benzylic product radical **2** that is more stable than **1** by 29 kJ/mol (Table 1). This difference is almost identical to what would be expected for the difference in radical stabilization through two methyl groups as compared to one phenyl group.[21] The influence of the phosphate group on the stability difference between radicals **1** and **2** therefore appears to be only minor. Structural features of **2** include a practically planar radical center in almost perfect conjugation with the aryl ring system and a newly formed C−O bond of 1.49 Å length. The unpaired spin density is not only located at the benzylic position (0.68) but also delocalizes into the aromatic π-system. The dimethyl phosphate group of **2** carries practically no unpaired spin density, but an overall negative charge of −0.38.

The most favorable reaction pathway from radical **1** to **2** leads through three-membered ring transition state **3**, located +23.9 kJ/mol above **1**. This transition state can be classified as "early"

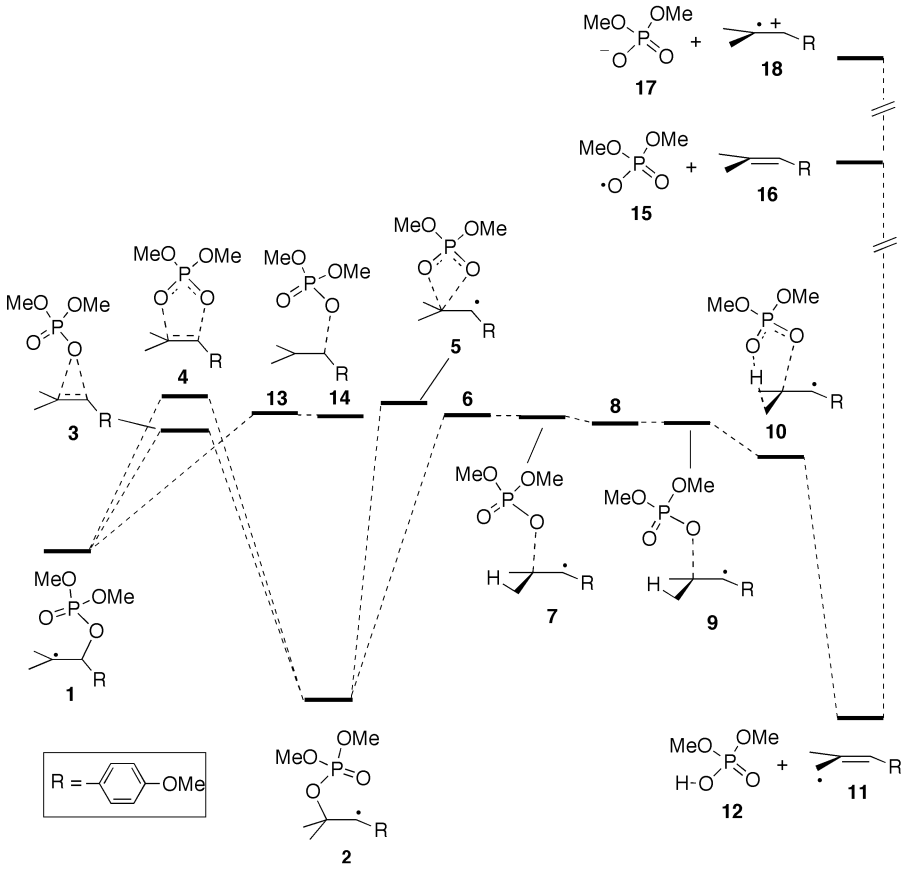

Figure 1. Reaction pathways in rearrangement reactions of radical **1** (drawn to sale at the B3LYP/LB level of theory).

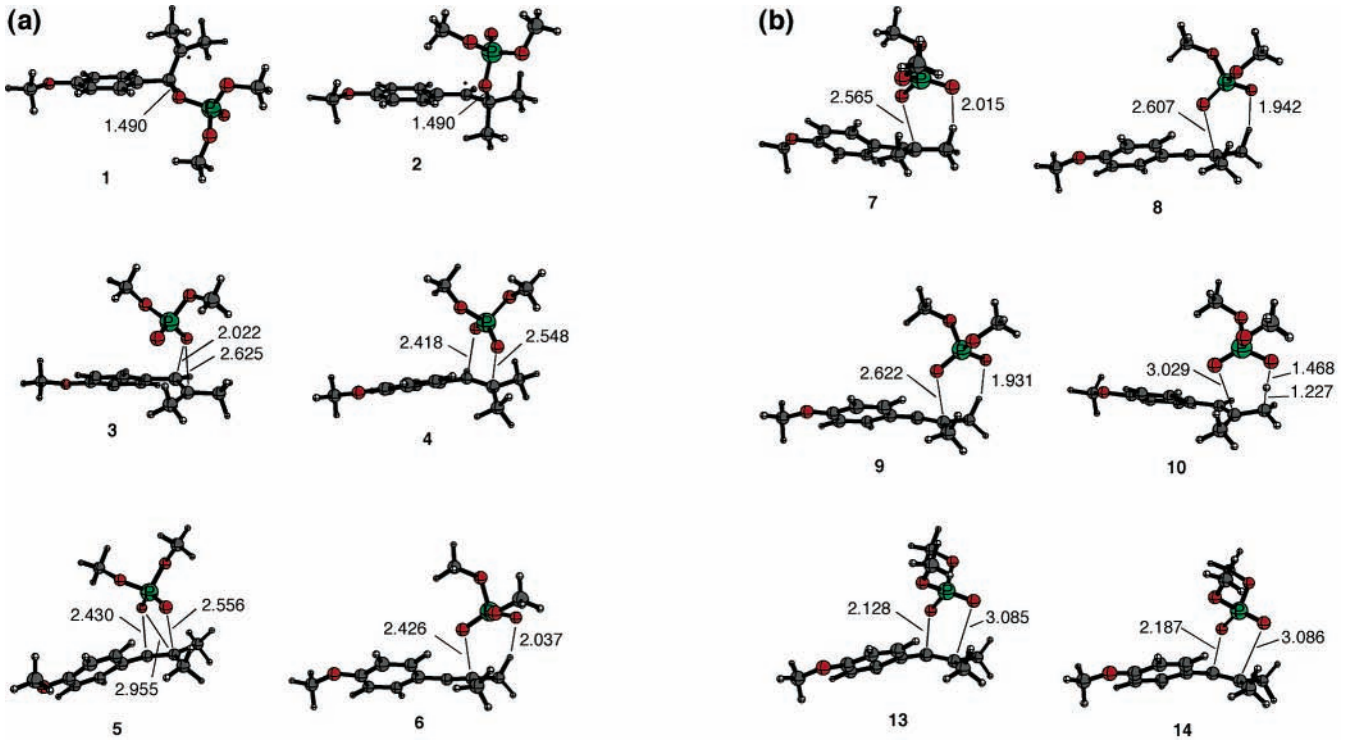

Figure 2. (a) Stationary points **1**−**6** on the potential energy surface of 2-(dimethylphosphatoxy)-2-(*p*-methoxyphenyl)-1,1-dimethylethyl radical (**1**) as optimized at the Becke3LYP/6-31G(d) level of theory. (b) Stationary points **7**−**14** on the potential energy surface of 2-(dimethylphosphatoxy)-2-(*p*-methoxyphenyl)-1,1-dimethylethyl radical (**1**) as optimized at the Becke3LYP/6-31G(d) level of theory.

in that the length of the breaking bond of 2.02 Å is significantly shorter than that of the forming bond of 2.63 Å. The electronic characteristics of this migration reaction can be described as "mixed homolytic/heterolytic" in that the overall charge (−0.55) as well as the overall spin density (0.28) of the phosphate group is significantly larger than in the ground-state radical **1**.

A second concerted rearrangement pathway leads through five-membered ring transition state **4**, located +29.9 kJ/mol

TABLE 1: Relative Energies at 298 K for Stationary Points in the Reaction of Radical 1 [in kJ/mol]

	gas phase		THF		CH_3CN	
structure	B3LYP/LB	BHLYP/LB	B3LYP/LB	BHLYP/LB	B3LYP/LB	BHLYP/LB
1	0.0	0.0	0.0	0.0	0.0	0.0
2	−28.7	−30.9	−31.1	−33.3	−31.6	−33.8
3	+23.9	+52.4	+17.6	+46.1	+15.6	+44.1
4	+29.9	+58.8	+16.5	+45.4	+13.7	+42.6
5	+28.2	+56.9	+16.0	+44.7	+13.4	+42.1
6	+26.0	+61.1	+6.5	+41.6	+3.2	+38.3
7	+25.3	+62.8	+5.3	+42.8	+2.4	+39.9
8	+24.2	+61.8	+3.8	+41.4	+0.4	+38.0
9	+24.2	+61.8	+3.8	+41.4	+0.4	+38.0
10	+17.9	+59.8	+2.0	+43.9	+0.4	+42.3
11 + 12	−32.2	−15.7	−50.5	−34.0	−46.9	−30.4
13	+26.6	+57.3	+16.8	+47.5	+14.0	+44.7
14	+25.9	+57.9	+15.3	+47.3	+12.9	+44.9
15 + 16	+72.1	+114.9	+56.5	+99.3	+61.3	+104.1
17 + 18	+367.7	+404.7	+43.8	+80.8	+6.3	+43.3

TABLE 2: Cumulative Phosphate Group Charges and Phosphate Group Spin Densities (NPA Values) for Stationary Points in the Reaction of Radical 1 as Calculated at the B3LYP/6-31G(d) Level [in au]

	gas phase		THF		CH_3CN	
structure	q (PO_4Me_2)	spin density (PO_4Me_2)	q (PO_4Me_2)	spin density (PO_4Me_2)	q (PO_4Me_2)	spin density (PO_4Me_2)
1	−0.366	0.060	−0.369	0.060	−0.370	0.060
2	−0.377	0.028	−0.382	0.027	−0.384	0.027
3	−0.549	0.283	−0.581	0.256	−0.588	0.250
4	−0.698	0.197	−0.745	0.156	−0.754	0.148
5	−0.704	0.193	−0.750	0.153	−0.758	0.145
6	−0.647	0.266	−0.722	0.195	−0.736	0.181
7	−0.642	0.293	−0.732	0.204	−0.732	0.204
8	−0.649	0.286	−0.747	0.188	−0.766	0.170
9	−0.650	0.285	−0.750	0.186	−0.769	0.167
10	−0.676	0.171	−0.731	0.120	−0.739	0.112
12	−0.478		−0.467		−0.465	
13	−0.590	0.296	−0.629	0.257	−0.639	0.249
14	−0.599	0.306	−0.645	0.261	−0.655	0.251

above **1**. With a breaking bond distance of 2.42 Å and a forming bond distance of 2.55 Å transition state **4** has much more dissociative character than **3**. The phosphate group in **4** is more negative than in **3** at −0.70, while carrying somewhat less spin density (0.20). A third transition state **5** for a concerted process has been identified that starts and ends at product radical **2**. Through this reaction pathway the two phosphate oxygen atoms not connected to methyl groups exchange their positions. Transition states **4** and **5** are rather similar energetically as well as structurally (Figure 2) and also show similar degrees of charge and spin density distribution. However, calculation of the intrinsic reaction pathways leaves no doubt that transition state **5** does not connect directly to reactant radical **1**. Considering the very flat potential energy surface (reflected through imaginary frequencies of 131 cm^{-1} for **5** and 134 cm^{-1} for **4**) this result may, however, be strongly dependent on the choice of the coordinate system.[22]

All attempts to localize transition states for the syn-1,3 elimination of phosphate (Scheme 1, pathway c) indicate that, in contrast to the smaller model systems investigated earlier, phosphate elimination occurs in a stepwise manner from radical **1** as well as **2**. Moreover, the rather flat potential energy surface for this process features multiple minima differing from each other through reorientation of the phosphate group. A typical sequence for the elimination process is described by stationary points **6**−**12** (Figure 1). Cleavage of the C−O bond in radical **2** through transition state **6** yields a first intermediate complex **7** in an endothermic reaction. This is followed by phosphate group reorientation through transition state **8** and yields a second complex **9**. Attack of the phosphate group at one of the methyl C−H bonds through transition state **10** yields allylic radical **11** and dimethyl phosphate **12** as the final products. This sequence of stationary points is located on a rather flat potential energy surface, the energetically most demanding step being the initial C−O bond cleavage step with a barrier of +26.0 kJ/mol relative to **1**. This bond cleavage process cannot be classified strictly as homolytic or heterolytic as the resulting complex **7** is characterized by a phosphate group charge of −0.64 and a phosphate group spin density of 0.29. Rather similar results are obtained for complex **9**. Still these two intermediates can best be understood as contact radical ion pairs. This characterization is quite independent of the population analysis method used as the Mulliken population analysis scheme predicts rather similar charge and spin density distributions as does the NPA scheme (see Supporting Information). Variation of the basis set also has only minor consequences.[23]

The flat surface described by structures **6** through **10** can also be reached through transition state **13**, located 26.6 kJ/mol above **1**. The product complex **14** formed in this process is structurally quite different from complexes **7** or **9** but shares their electronic characteristics in that the phosphate group carries a substantial negative charge as well as an increased spin density (Table 2).

Aside from the formation of rearranged benzylic radical **2** and dimethyl phosphate elimination to yield allylic radical **11**, two additional product channels exist. These include (a) the homolytic C−O bond cleavage in **1** yielding dimethyl phosphate radical **15** and styrene **16** and (b) the heterolytic C−O bond cleavage in **1** yielding dimethyl phosphate anion **17** and styrene radical cation **18**. The homolytic pathway is endothermic by +72.1 kJ/mol and thus energetically much less favorable than the other pathways described above. Heterolysis is even less favorable in the absence of a reaction medium and is endo-

TABLE 3: Vertical Optical Transitions for Stationary Points 2, 9, 11, and 18 as Calculated at the TDDFT/UB3LYP/6-311+G(d,p)//B3LYP/6.31G(d) and CC2 Level of Theory Together with Selected Experimental Data[a]

	TDDFT/Becke3LYP			CC2		exptl
structure	λ [nm]	f	transition, (spin)	λ [nm]	f	λ [nm]
2	410	0.007	π(HOMO)/π^*(LUMO), (α)	344	0.012	310−320[b]
	392	0.017	π(HOMO)/π^*(LUMO), (β)	336	0.017	
	326	0.014	π(HOMO − 1)/π^*(LUMO), (β)	268	0.026	
	296	0.210	π(HOMO)/σ^*(LUMO + 1), (α)	262	0.207	
	308	0.001	π(HOMO − 1)/π^*(LUMO), (α)	246	0.385	
9	919	0.124	LP(HOMO)/π^*(LUMO), (β)	992	0.180	
	1042	0.005	LP(HOMO − 2)/π^*(LUMO), (β)	867	0.013	
	610	0.009	LP(HOMO − 1)/π^*(LUMO), (β)	639	0.007	
	804	0.021	(HOMO − 3)/π^*(LUMO), (β)	556	0.018	
	545	0.012	(HOMO − 3)/π^*(LUMO), (β)	490	0.101	
11	450	0.009	HOMO/π^*(LUMO + 1), (α)	369	0.005	354[c]
	409	0.006	HOMO/π^*(LUMO), (α)	329	0.012	
	324	0.146	π(HOMO − 1)/π^*(LUMO), (β)	278	0.070	
	314	0.449	π(HOMO − 2)/π^*(LUMO), (β)	270	0.782	
	318	0.154	π(HOMO)/π^*(LUMO + 1), (α)			
18	622	0.006	π(HOMO − 1)/π^*(LUMO), (β)	554	0.085	600−700[d]
	555	0.128	π(HOMO)/π^*(LUMO), (β)	525	0.112	
	340	0.559	π(HOMO − 2)/π^*(LUMO + 1), (β)	337	0.763	390[d]
	342	0.023	π(HOMO)/π^*(LUMO), (α)			
	308	0.009	π(HOMO)/π^*(LUMO), (α)	305	0.0002	

[a] Only the five lowest energy transitions are given. The state ordering is based on the CC2 results. [b] In THF; see ref 4. [c] In CH_3CN; see ref 4. [d] In CH_3CN; see ref 4.

thermic by 367.8 kJ/mol. The concerted rearrangement through transition state **3** yielding benzylic radical **2** therefore remains as the kinetically most favorable reaction pathway, closely followed by formation of a contact radical ion pair (CRIP) **7** through transition state **6**. Analysis of the BHLYP/LB instead of the B3LYP/LB barriers leads to much the same conclusion, despite the fact that the absolute reaction barriers are significantly higher at the former level of theory. Unfortunately, neither the B3LYP/LB nor the BHLYP/LB gas-phase reaction barriers can easily be reconciled with the experimentally measured activation energy in THF as the former is too low and the latter too high. The additional consideration of solvent effects is necessary in this case to improve the situation (see below).

Spectroscopic Properties of Selected Intermediates. The detection of reaction intermediates and products through time-resolved UV spectroscopy has provided much of the quantitative reactivity data for β-phosphatoxyalkyl radicals. Still, the direct experimental detection of contact radical ion pairs has not yet been achieved. As prediction of a UV spectrum of these intermediates may aid their ultimate experimental detection, we have used TDDFT[13] and coupled-cluster type response (CC2)[17,19] methods here to calculate the vertical electronic excitation spectrum for intermediates such as **9**. TDDFT has recently developed into a useful tool for the prediction of UV spectra of larger molecular systems whose size precludes application of more sophisticated methods. Application of TDDFT theory to small[24−27] and large[14,24,28] open shell systems is a relatively new field. Good results have previously been obtained[24,28] using basis sets as small as 6-31+G(d) or 6-311+G(d,p), and we will therefore make use of the latter, here in combination with the UBecke3LYP hybrid functional. Previous results suggest that this combination predicts low-energy electronic transitions in neutral radicals that are blue-shifted relative to the experimentally measured spectra by 10−30 nm (corresponding to 0.10−0.19 eV in the spectral region around 400 nm). The relatively new CC2 method, in contrast, has not yet been tested thoroughly for the prediction of excited states of radicals, but experience[29] for closed shell compounds indicates that CC2 is as accurate as TDDFT/B3LYP and probably superior for charged open shell systems where DFT is known to be problematic.[30] Perusal of experimental data starts with the UV−vis spectrum of benzylic radical **2** featuring a strong transition at 300−320 nm in THF or acetonitrile as the solvent.[4e] Similar results have been reported for other benzylic radicals.[4f] The theoretically (CC2) calculated spectrum features a weak absorption at around 340 nm and a much stronger band at 262 nm which is in reasonable agreement with the experimental data, whereas TDDFT/B3LYP predicts the same bands red-shifted by about 60 and 50 nm (0.5−0.6 eV), respectively. Time-resolved UV−vis spectra for styrene radical cation **18** have been measured by Newcomb et al.[4e] Aside from a broad, poorly resolved absorption in the region between 600 and 700 nm the most characteristic absorption band for **18** is centered at around 390 nm. Similar results have been reported for 4-methoxystyrene radical cations lacking one of the terminal methyl groups in **18**.[31]

The CC2 method yields two transitions at 554 and 525 nm, respectively, with medium intensity and a stronger transition at 390 nm, which can be assigned to the two experimentally observed bands. The blue-shift of the theoretical excitation energies compared to the experimental values of about 0.4−0.5 eV can be explained by solvent effects which are expected to be more relevant for cations than for neutral systems (e.g., **2**). The results from the TDDFT treatment are very similar except that an additional state at 342 nm not found with CC2 is obtained. No direct experimental evidence is available for allylic radical **11**, but UV spectra have been measured for related allyl radicals. Scaiano et al. have reported[32] a characteristic absorption around 360 nm for the 1,3-diphenylallyl radical in cyclohexane as the solvent, and a similar value of 354 nm has been found for the 2-benzyl-1,3-diphenylallyl radical in acetonitrile by Newcomb et al.[4f] If we adopt this latter value as being typical for aryl-substituted allyl radicals such as **11** and compare it to the first (weak) absorptions of 369 and 329 nm predicted with the CC2 method (Table 3), we note again that the excitation energies are predicted quite accurately. The calculated electronic excitation spectrum predicted for contact radical ion pair **9** differs from those for radicals **2**, **11**, and **18** in two major points. First, two very long wavelength absorptions at 992 nm and

(weaker) at 867 nm are predicted for **9** that are far away from the main absorptions for the other radicals, putting **9** into a spectral range that may not even be accessible in experiments designed for the investigation of **2**, **11**, and **18**. Second, whereas the low-energy excitations in radicals **2**, **11**, and **18** exclusively involve the π-orbitals of the styrene moiety contained in these systems, the long wavelength absorptions predicted for **9** derive from excitations of lone pair electrons of the phosphate group into the unoccupied π*-orbitals of the styrene moiety. The finding that two different quantum chemical methods predict similar long wavelength absorption bands for **9** gives some confidence to the reliability of the theoretical models. Both the predicted absorption bands for **9** as well as the different electronic characteristics of the excitation itself suggest, however, that the UV−vis characteristics of radical cation **18** and its contact ion pairs will be dramatically different in the absence of specific solvent effects.

Reaction of Radical 1 in Organic Solvents. There is overwhelming experimental evidence that the reaction of radicals such as **1** follows a heterolytic pathway in polar media such as water or acetonitrile/water mixtures.[1−4] Whether the reaction proceeds along the same lines also in organic solvents such as tetrahydrofuran (THF, $\epsilon = 7.6$) or pure acetonitrile (CH_3CN, $\epsilon = 36.6$) is more difficult to assess. We have therefore explored solvent effects in these media using single-point calculations with the PCM solvation model.[15] The reaction barriers in THF are significantly lower than those calculated for the gas phase, the effects being particularly large for the stepwise pathways leading through CRIPs. Inspection of the B3LYP/LB results for THF in Table 1 reveals that 1,2-migration through transition state **3** and cleavage of the C−O bond through transition state **13** face practically identical barriers. However, the calculated absolute reaction barriers appear to be unreasonably low for practically all pathways, and it appears that the combination of BHLYP/LB gas-phase energies with PCM solvation free energies gives a somewhat more reliable picture. At this latter level the reaction barriers for migration of the phosphate groups through transition state **3** and for heterolytic C−O bond cleavage through transition state **13** are again rather similar and only slightly higher than the experimentally determined value of $+40.6 \pm 5$ kJ/mol for reaction of the diethyl phosphate ester.[4e] Heterolytic cleavage to yield the ionic fragments **17** and **18** is thermochemically more favorable now than homolytic cleavage to yield the neutral fragments **15** and **16**. Formation of two separate fragments remains, however, much less favorable than that of neutral products or formation of CRIPs such as **7**, **9**, or **14**. Reaction barriers calculated for acetonitrile as a medium are uniformly lower than those calculated for THF (Table 1). The actual barrier lowering for the most important processes through transition states **3** and **13** of around 3 kJ/mol is, however, rather moderate when compared to the experimentally determined lowering of the reaction barrier by 15 kJ/mol. The discrepancy may be due to the use of gas-phase geometries, neglecting effects of structural relaxation especially in more polar solvents.[33] This latter relaxation may also be responsible for the differences in experimentally measured log *A* terms observed in THF and acetonitrile.

The very small energy difference between CRIP **14** and transition state **13** of less than 2 kJ/mol even in THF or acetonitrile solution has important consequences for the chances of detecting CRIPs in general. If the barriers for recombination to reactant **1** or product **2** are indeed on the order of only a few kJ/mol, the lifetime of these intermediates will be very limited and picosecond to femtosecond laser spectroscopic techniques may be required for their detection.

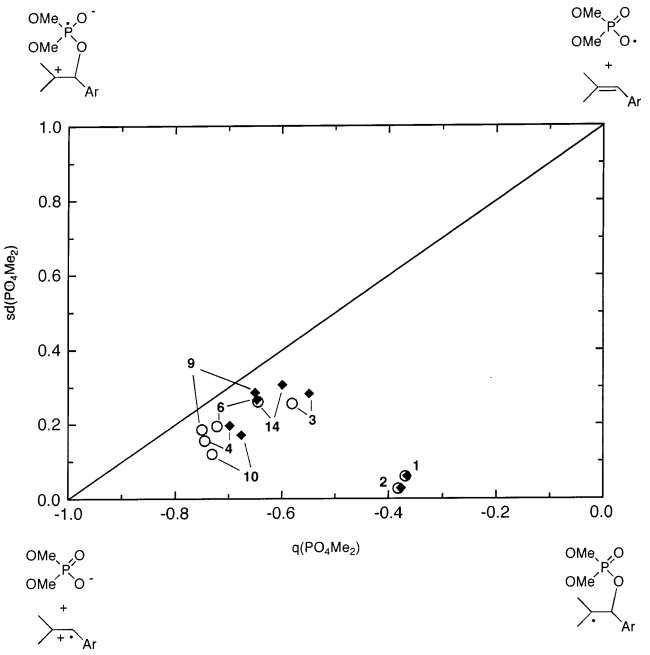

Figure 3. Phosphate group spin densities and phosphate group electron densities as calculated at the Becke3LYP/6-31G(d) level of theory using the NPA scheme. Gas-phase values are shown in filled diamonds, THF values in open circles.

Discussion

The discussion of the heterolytic, concerted or even homolytic character of 1,2-migration reactions in β-(phosphatoxy)alkyl radicals has always been difficult because of a lack of quantitative data on the charge distribution present along different reaction pathways. Although the observation of solvent effects can certainly be interpreted as support for a charge-separate transition state or even an ion pair intermediate, the actual degree of charge separation cannot be determined directly from these experiments. Direct detection of diffusively free radical cations such as **18** or phosphate anions such as **17** is reliable proof for a heterolytic reaction in some of the reaction media, but the character of the hypothetical CRIPs in less polar media remains elusive. It is one of the more interesting observations of this theoretical study that not only the transition states but also the intermediates identified on the potential energy surface of **1** have phosphate group charges far from −1.0, even in THF solution (Table 2). The most negatively charged phosphate group is present in intermediate **9** at −0.75. One implication of the nonintegral charge separation in a CRIP such as **9** is that the spectroscopic properties of the two nascent fragments are likely to be different from those of the separate fragments. Spectroscopic detection of contact radical ion pairs might therefore not be possible at the (known) wavelengths of the separate fragments. The data in Table 2 can be appreciated much better in a graphical representation in which the phosphate group charge is plotted against the phosphate group spin density (sdq plot) together with the limiting cases of a fully heterolytic or fully homolytic C−O bond cleavage (Figure 3). Such a presentation can be thought of as an electronic More O'Ferrall−Jencks diagram, as it depicts the electronic (and not the molecular) structure of reactants, products, and intermediates.[34,35] To limit the complexity of the sdq plot only the most important stationary points described in Table 2 have been included. Also, the values

calculated for THF and acetonitrile are so similar that only the former are shown. The four corners of Figure 3 are occupied by the four most relevant electronic configurations. In the lower right is the configuration describing a purely covalent C−O bond with a phosphate group charge and spin density of exactly zero, in the lower left corner is the configuration describing heterolytic C−O bond cleavage, and in the upper right corner is the configuration describing homolytic C−O bond cleavage. The upper left corner must then be occupied by an electronic configuration in which the phosphate group carries both a full negative charge as well as all of the unpaired spin density. The location of reactant radical **1** and product radical **2** at the bottom of Figure 3 indicates that the heterolytic configuration in the lower left corner contributes substantially to the description of these two ground-state structures. All other stationary points (transition states and CRIPs) are located to the upper left of radicals **1** and **2**, indicating an increase in the phosphate group charge as well as spin density. This implies that even formation of the CRIPs **7**, **8**, and **14** involves a partially homolytic component not reflected in their designation. The presence of a solvent reaction field has little influence on the characteristics of the ground states **1** and **2** but moves all other stationary points toward the lower left corner, along the diagonal connecting the fully heterolytic with the fully homolytic electronic configurations. This solvent-induced shift is particularly large for CRIP **9** and transition state **6**.

In conclusion, the unimolecular chemistry of β-(phosphatoxy)-alkyl radical **1** has been found to be of mixed homolytic/heterolytic character with a dominating heterolytic component. Aside from concerted reaction pathways for 1,2-migration of the phosphate group, a flat region of the potential energy surface has been identified that contains intermediates of nonintegral charge separation. This region of the potential energy surface can be reached from the reactant radical **1** as well as the rearranged radical **2** or the phosphoric acid elimination products **11** and **12**. The intermediates located on this part of the potential energy surface can best be understood as contact radical ion pairs based on their overall geometrical structure. The nonclassical electronic structure of these intermediates might, together with the minimal barrier for their collapse to products, be responsible for the difficulties involved in their experimental detection and characterization. The absolute reaction barriers are strongly influenced through the presence of a solvent reaction field even for a low-polarity solvent such as THF and thus show the expected behavior for a charge-separating reaction type.

Acknowledgment. This manuscript is dedicated to Professor Helmut Schwarz on the occasion of his 60th birthday. Financial support for this study obtained from the Volkswagenstiftung and the Fonds der Chemischen Industrie is gratefully acknowledged. We thank Professor V. Barone for helpful discussions and technical assistance.

Supporting Information Available: Energies and structures of all stationary points described in this paper. This material is available free of charge via the Internet at http://pubs.acs.org.

References and Notes

(1) (a) Beckwith, A. L. J.; Crich, D.; Duggan, P. J.; Yao, Q. *Chem. Rev.* **1997**, *97*, 3273. (b) Knapp-Pogozelski, W.; Tullius, T. D. *Chem. Rev.* **1998**, *98*, 1089. (c) Breen, A. P.; Murphy, J. A. *Free Radical Biol. Med.* **1995**, *18*, 1032.

(2) (a) Dizdaroglu, M.; von Sonntag, C.; Schulte-Frohlinde, D. *J. Am. Chem. Soc.* **1975**, *97*, 2277. (b) Behrens, G.; Koltzenburg, G.; Ritter, A.; Schulte-Frohlinde, D. *Int. J. Radiat. Biol.* **1978**, *33*, 163. (c) Koltzenburg, G.; Behrens, G.; Schulte-Frohlinde, D. *J. Am. Chem. Soc.* **1982**, *104*, 7311.

(3) (a) Glatthaar, R.; Spichty, M.; Gugger, A.; Batra, R.; Damm, W.; Mohr, M.; Zipse, H.; Giese, B. *Tetrahedron* **2000**, *56*, 4117. (b) Meggers, E.; Dussy, A.; Schäfer, T.; Giese, B. *Chem.—Eur. J.* **2000**, *6*, 485. (c) Gugger, A.; Batra, R.; Rzadek, P.; Rist, G.; Giese, B. *J. Am. Chem. Soc.* **1997**, *119*, 8740. (d) Giese, B.; Beyrich-Graf, X.; Erdmann, P.; Petretta, M.; Schwitter, U. *Chem. Biol.* **1995**, *2*, 367. (e) Giese, B.; Beyrich-Graf, X.; Burger, J.; Kesselheim, C.; Senn, M.; Schäfer, T. *Angew. Chem., Int. Ed. Engl.* **1993**, *32*, 1742.

(4) (a) Newcomb, M.; Miranda, N.; Sannigrahi, M.; Huang, X.; Crich, D. *J. Am. Chem. Soc.* **2001**, *123*, 6445. (b) Horner, J. H.; Newcomb, M. *J. Am. Chem. Soc.* **2001**, *123*, 4364. (c) Bales, B. C.; Horner, J. H.; Huang, X.; Newcomb, M.; Crich, D.; Greenberg, M. M. *J. Am. Chem. Soc.* **2001**, *123*, 3623. (d) Newcomb, M.; Miranda, N.; Huang, X.; Crich, D. *J. Am. Chem. Soc.* **2000**, *122*, 6128. (e) Whitted, P. O.; Horner, J. A.; Newcomb, M.; Huang, X.; Crich, D. *Org. Lett.* **1999**, *1*, 153. (f) Newcomb, M.; Horner, J. H.; Whitted, P. O.; Crich, D.; Huang, X.; Yao, Q.; Zipse, H. *J. Am. Chem. Soc.* **1999**, *121*, 10685. (g) Choi, S.-Y.; Crich, D.; Horner, J. H.; Huang, X.; Martinez, F. N.; Newcomb, M.; Wink, D. J.; Yao, Q. *J. Am. Chem. Soc.* **1998**, *120*, 211.

(5) (a) Crich, D.; Ranganathan, K. *J. Am. Chem. Soc.* **2002**, *124*, 12422. (b) Crich, D.; Neelamkavil, S. *Org. Lett.* **2002**, *4*, 2573. (c) Crich, D.; Ranganathan, K.; Huang, X. *Org. Lett.* **2001**, *3*, 1917. (d) Crich, D.; Huang, X.; Newcomb, M. *J. Org. Chem.* **2000**, *65*, 523. (e) Crich, D.; Huang, X.; Newcomb, M. *Org. Lett.* **1999**, *1*, 225.

(6) Zipse, H. *J. Am. Chem. Soc.* **1997**, *119*, 2889.

(7) Becke, A. D. *J. Chem. Phys.* **1993**, *98*, 5648.

(8) Lee, C.; Yang, W.; Parr, R. G. *Phys. Rev. B* **1988**, *37*, 785.

(9) Becke, A. D. *J. Chem. Phys.* **1993**, *98*, 1372.

(10) (a) Lynch, B. J.; Fast, P. L.; Harris, M.; Truhlar, D. G. *J. Phys. Chem. A* **2000**, *104*, 4811. (b) Lynch, B. J.; Truhlar, D. G. *J. Phys. Chem. A* **2001**, *105*, 2936.

(11) Reed, A. E.; Curtiss, L. A.; Weinhold, F. *Chem. Rev.* **1988**, *88*, 899.

(12) A comparison of population analysis schemes for DFT calculations on open shell systems has been performed in: Zipse, H.; Bootz, M. *J. Chem. Soc., Perkin Trans. 2*, **2001**, 1566.

(13) (a) Bauernschmitt, R.; Ahlrichs, R. *Chem. Phys. Lett.* **1996**, *256*, 454. (b) Stratmann, R. E.; Scuseria, G. E.; Frisch, M. J. *J. Chem. Phys.* **1998**, *109*, 8218.

(14) Haselbach, E.; Allan, M.; Bally, T.; Bednarek, P.; Sergenton, A.-C.; de Meijere, A.; Kozhushkov, S.; Piacenza, M.; Grimme, S. *Helv. Chim. Acta* **2001**, *84*, 1670.

(15) (a) Barone, V.; Cossi, M.; Tomasi, J. *J. Chem. Phys.* **1997**, *107*, 3210. (b) Barone, V.; Cossi, M. *J. Phys. Chem. A* **1998**, *102*, 1995. (c) Amovilli, C.; Barone, V.; Cammi, R.; Cances, E.; Cossi, M.; Mennucci, B.; Pomelli, C. S.; Tomasi, J. *Adv. Quantum Chem.* **1998**, *32*, 227.

(16) Frisch, M. J.; Trucks, G. W.; Schlegel, H. B.; Scuseria, G. E.; Robb, M. A.; Cheeseman, J. R.; Zakrzewski, V. G.; Montgomery, J. A., Jr.; Stratmann, R. E.; Burant, J. C.; Dapprich, S.; Millam, J. M.; Daniels, A. D.; Kudin, K. N.; Strain, M. C.; Farkas, O.; Tomasi, J.; Barone, V.; Cossi, M.; Cammi, R.; Mennucci, B.; Pomelli, C.; Adamo, C.; Clifford, S.; Ochterski, J.; Petersson, G. A.; Ayala, P. Y.; Cui, Q.; Morokuma, K.; Malick, D. K.; Rabuck, A. D.; Raghavachari, K.; Foresman, J. B.; Cioslowski, J.; Ortiz, J. V.; Stefanov, B. B.; Liu, G.; Liashenko, A.; Piskorz, P.; Komaromi, I.; Gomperts, R.; Martin, R. L.; Fox, D. J.; Keith, T.; Al-Laham, M. A.; Peng, C. Y.; Nanayakkara, A.; Gonzalez, C.; Challacombe, M.; Gill, P. M. W.; Johnson, B. G.; Chen, W.; Wong, M. W.; Andres, J. L.; Head-Gordon, M.; Replogle, E. S.; Pople, J. A. *Gaussian 98*, revision A.7; Gaussian, Inc.: Pittsburgh, PA, 1998. All solvent effect data have been calculated using revision A.11.3.

(17) Christiansen, O.; Koch, H.; Jørgensen, P. *Chem. Phys. Lett.* **1995**, *243*, 409.

(18) Hättig, C.; Weigend, F. *J. Chem. Phys.* **2000**, *113*, 5154.

(19) Ahlrichs, R.; Bär, M.; Baron, H.-P.; Bauernschmitt, R.; Blöcker, S.; Ehrig, M.; Eichkorn, K.; Elliott, S.; Furche, F.; Haase, F.; Häser, M.; Horn, H.; Huber, C.; Huniar, U.; Kattannek, M.; Kölmel, C.; Kollowitz, M.; May, K.; Ochsenfeld, C.; Öhm, H.; Schäfer, A.; Schneider, U.; Treutler, O.; von Arnim, M.; Weigend, F.; Weis, P.; Weiss, H. *Turbomole*, version 5.6; Universität Karlsruhe, 2003.

(20) Schäfer, A.; Huber, C.; Ahlrichs, R. *J. Chem. Phys.* **1994**, *100*, 5829.

(21) Henry, D. J.; Parkinson, C. J.; Mayer, P. M.; Radom, L. *J. Phys. Chem. A* **2001**, *105*, 6750.

(22) (a) Sastry, G. N.; Danovich, D.; Shaik, S. *Angew. Chem., Int. Ed. Engl.* **1996**, *35*, 1098. (b) Bertran, J.; Gallardo, I.; Moreno, M.; Saveant, J.-M. *J. Am. Chem. Soc.* **1996**, *118*, 5737. (c) Sastry, G. N.; Shaik, S. *J. Phys. Chem.* **1996**, *100*, 12241. (d) Haik, S.; Danovich, D.; Sastry, G. N.; Ayala, P. Y.; Schlegel, H. B. *J. Am. Chem. Soc.* **1997**, *119*, 9327. (e) Bakken, V.; Danovich, D.; Shaik, S.; Schlegel, H. B. *J. Am. Chem. Soc.* **2001**, *123*, 130.

(23) Because of problems with the NPA scheme, this point has only been explored with the Mulliken population analysis. The following

phosphate group charges have been calculated using the B3LYP functional in combination with a selection of basis sets for intermediate **7**: −0.587 [6-31G(d)]; −0.581 [6-31+G(d)]; −0.610 [6-31+G(d, p)]; −0.630 [6-31++G(d, p)]; −0.538 [6-311+G(d, p)]; −0.509 [6-311+G(2d, p)]; −0.504 [cc-pVDZ]; −0.592 [cc-pVTZ].

(24) (a) Hirata, S.; Head-Gordon, M. *Chem. Phys. Lett.* **1999**, *302*, 375. (b) Weisman, J. L.; Head-Gordon, M. *J. Am. Chem. Soc.* **2001**, *123*, 11686.

(25) Spielfiedel, A.; Handy, N. C. *Phys. Chem. Chem. Phys.* **1999**, *1*, 2401.

(26) Guan, J.; Casida, M. E.; Salahub, D. R. *J. Mol. Struct. (THEOCHEM),* **2000**, *527*, 229.

(27) Broclawik, E.; Borowski, T. *Chem. Phys. Lett.* **2001**, *339*, 433.

(28) (a) Chatgilialoglu, C.; Ferreri, C.; Bazzanini, R.; Guerra, M.; Choi, S.-Y.; Emanuel, C. J.; Horner, J. H.; Newcomb, M. *J. Am. Chem. Soc.* **2000**, *122*, 9525. (b) Chatgilialoglu, C.; Guerra, M.; Mulazzani, Q. G. *J. Am. Chem. Soc.* **2003**, *125*, 3839.

(29) Parac, M.; Grimme, S. *J. Phys. Chem. A* **2002**, *106*, 6844.

(30) Gruening, M.; Gritsenko, O. V.; van Gisbergen, S. J. A.; Baerends, E. J. *J. Phys. Chem. A* **2001**, *105*, 9211.

(31) Johnston, L. J.; Schepp, N. P. *J. Am. Chem. Soc.* **1993**, *115*, 6564.

(32) Miranda, M. A.; Perez-Prieto, J.; Font-Sanchis, E.; Konya, K.; Scaiano, J. C. *J. Org. Chem.* **1997**, *62*, 5713.

(33) Geometry optimizations at the B3LYP/6-31G(d) level using the PCM continuum solvation model and THF as a solvent have been attempted but met with severe convergence problems.

(34) (a) More O'Ferrall, R. A. *J. Chem. Soc.* **1970**, 274. (b) Jencks, W. P. *Chem. Rev.* **1972**, *72*, 706.

(35) Zipse, H. *Adv. Phys. Org. Chem.* **2003**, *38*, 111.